Journal of Colloid and Interface Science 620 (2022) 346–355

Contents lists available at ScienceDirect

Journal of Colloid and Interface Science

journal homepage: www.elsevier.com/locate/jcis

A guide to designing graphene-philic surfactants

Tretya Ardyani [a], Azmi Mohamed [a,b,*], Suriani Abu Bakar [b], Masanobu Sagisaka [c], Mohamad Hafiz Mamat [d], Mohd Khairul Ahmad [e], Sofian Ibrahim [f], H.P.S. Abdul Khalil [g], Stephen M. King [h], Sarah E. Rogers [h], Julian Eastoe [i]

[a] Department of Chemistry, Faculty of Science and Mathematics, Universiti Pendidikan Sultan Idris, 35900 Tanjong Malim, Perak, Malaysia
[b] Nanotechnology Research Centre, Faculty of Science and Mathematics, Universiti Pendidikan Sultan Idris, 35900 Tanjong Malim, Perak, Malaysia
[c] Department of Frontier Materials Chemistry, Graduate School of Science and Technology, Hirosaki University, Bunkyo-cho 3, Hirosaki, Aomori 036-8561, Japan
[d] NANO-ElecTronic Centre (NET), School of Electrical Engineering, College of Engineering, Universiti Teknologi MARA, 40450 Shah Alam, Selangor, Malaysia
[e] Microelectronic and Nanotechnology – Shamsuddin Research Centre (MiNT-SRC), Faculty of Electrical and Electronic Engineering, Universiti Tun Hussein Onn Malaysia, 86400 Parit Raja, Batu Pahat, Johor, Malaysia
[f] Malaysian Institute for Nuclear Technology Research (MINT) Bangi, 43000 Kajang, Selangor, Malaysia
[g] School of Industrial Technology, Universiti Sains Malaysia, 11700 Gelugor, Penang, Malaysia
[h] Rutherford Appleton Laboratory, ISIS Spallation Source, Chilton, Oxfordshire OX110QT, United Kingdom
[i] School of Chemistry, University of Bristol, Cantock's Close, Bristol BS8 1TS, United Kingdom

GRAPHICAL ABSTRACT

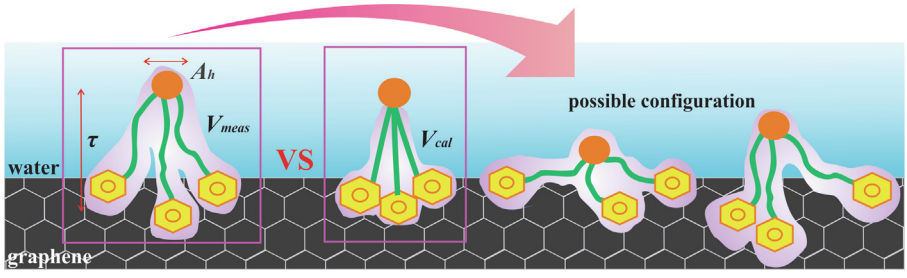

ARTICLE INFO

Article history:
Received 27 January 2022
Revised 30 March 2022
Accepted 31 March 2022
Available online 2 April 2022

Keywords:
Surface tension
Aggregation
Surfactant coverage
Graphene
Interfacial properties
Nanocomposites

ABSTRACT

Hypothesis: As compared to common aliphatic surfactants, increasing the number of pendant or incorporated aromatic groups in a surfactant is expected to offer significant enhancement in the affinity for graphene surfaces. The basis for enhanced graphene-philicity of aromatic surfactants is that they can develop appreciable $\pi - \pi$ interactions with graphene. Furthermore, charged (anionic) surfactants are expected to confer electrostatic stabilization on surfactant-graphene composites. Hence, it is expected that anionic aromatic surfactants combine these two properties for effective stabilization of graphene dispersions in water.

Experimental: The properties of two custom made graphene-compatible surfactants carrying two and three aromatic moieties in the hydrophobic tails, namely DC3Ph2 (sodium 1,4-dioxo-1,4-bis(3-phenylpropoxy)butane-2-sulfonate) and TC3Ph3 (sodium 1,5-dioxo-1,5-bis(3-phenylpropoxy)-3-((3-phenylpropoxy)carbonyl) pentane-2-sulfonate) were compared with other common ionic commercial surfactants. Air-water (a/w) surface tension measurements were used to assess the surfactant adsorption and interfacial packing in the absence and presence of graphene. The surfactant coverage index for graphene (Φ) was calculated using surfactant headgroup areas derived from a/w surface tension data, chain volumes, and molecular fragment volumes from literature.

* Corresponding author at: Department of Chemistry, Nanotechnology Research Centre, Faculty of Science and Mathematics, Universiti Pendidikan Sultan Idris, 35900 Tanjong Malim, Perak, Malaysia.
E-mail address: azmi.mohamed@fsmt.upsi.edu.my (A. Mohamed).

https://doi.org/10.1016/j.jcis.2022.03.145

Findings: Increasing the number of aromatic groups and tails per surfactant was shown to increase the ability of surfactants to pack and fill space, as expressed by Φ. Comparison between the values of Φ for surfactants of different chain structure and architecture showed that the affinity for graphene increased with Φ. Hence, there is an implicit link between surfactant-graphene compatibility and the identity, chemical composition and architecture of the surfactant chains.

1. Introduction

Stable graphene dispersions and nanocomposites are of interest for many potential applications [1], however, there still are limitations to the current methods used to stabilize hydrophobic graphene in aqueous phases [2]. Various experimental methods are employed to assess stabilities of these dispersions, such as spectroscopic or electrophoretic mobility measurements [1,3,4]. Over recent years, different surfactants have been tested with the aim to identify the most effective types and chemical structures for exfoliating and stabilizing graphene dispersions [5–7,8]. The essential role of surfactant architecture is now appreciated [9,10], in particular the presence of aromatic ring(s) in the surfactant chains has been shown to greatly improve the stability of graphene dispersions either in aqueous phases or polymer matrices [6,7,10,11]. The study of graphene/polymer nanocomposites was pioneered by Tkalya et al. who employed poly(sodium-4-styrenesulfonate) as a stabilizer [12], demonstrating stability against graphene agglomeration for up to a year. In other studies, the common surfactant sodium dodecylbenzenesulfonate (SDBS, bearing one aromatic ring, close to the hydrophilic headgroup) has been shown to confer stability on graphene dispersions and gives low percolation thresholds (0.3 wt%) for the nanocomposites [13,14].

Recently, the use of stabilizers bearing extensive aromatic moieties e.g. pyrene and its derivatives, has been demonstrated by a number of research groups. An et al. applied 1-pyrenecarboxylic acid to exfoliate graphite into aqueous dispersions of graphene, offering stabilities similar to micromechanical exfoliation [15]. Parviz et al. highlighted that pyrene derivatives can lead to higher graphene loadings, as compared to SDBS [5]. Shin et al. employed very hydrophobic pyrene derivatives for exfoliating graphite [16], showing that stabilizers containing two pyrene groups offered improved exfoliation as well as enhanced dispersion stability (as indicated by higher zeta potentials).

The number of aromatic rings in the stabilizer molecules is important as it affects the extent of π-π interactions, which are at the heart of exfoliation, stabilization, and adsorption [17–19]. Although, to what extent aromatization is important is yet to be resolved. For that reason, understanding how to optimize surfactant architecture for enhanced graphene-compatibility is a central question still to be answered, and is addressed in this paper.

On a related front, in studies of microemulsion stabilities and properties, surfactant performance is linked to the surfactant molecular area at the interface a_o [20–22]. A useful parameter to assess an occupied volume is the critical packing parameter (CPP = $v_o/l_o a_o$) [23,24], with surfactant tail volume v_o and the effective length of the surfactant tail l_o. Based on this CPP approach, bulky surfactants will provide more efficient space filling, allowing less penetration of solvent into the interfacial region and enhanced stability of the oil–water interface [22,25]. Within this CPP framework, for linear chain surfactants, the ratio between v_o and l_o is assumed to be constant; therefore, a_o is the dominant parameter [26], helping guide the design of new optimized surfactants [6,20,27]. Chain branching, methylation, or other structural variations can be employed to optimize the surfactant structure further still [20,22]. Considering now surfactant-stabilized graphene dispersions, the links between surfactant architecture and dispersion stability have not yet been fully uncovered. In this respect, of special interest are those surfactants incorporating aromatic groups for promoting π-π interactions with graphene. Considering that structural modifications will affect the "bulkiness" of surfactants, it might be thought that that π-π interactions may be not the whole story.

This paper introduces a predictive index Φ, related to CPP, to characterize the packing density of adsorbed surfactant layers in graphene dispersions (Eq. (1)). As such, this coverage parameter is more general than CPP and is appropriate for linking to graphene dispersion stability.

This surfactant coverage index Φ is.

$$\Phi = \frac{V_{cal}}{V_{meas}} \tag{1}$$

where V_{cal} is the calculated physical volume of the surfactant molecular fragments, whereas V_{meas} (=$l_o a_o$) is the experimentally determined total surfactant volume at the air–water interface. As such Φ has previously been used to evaluate performance of fluorinated surfactants for stabilizing water-in-CO_2 (w/CO_2) microemulsions [21,28]. In line with results from simulation studies [25], modifying surfactant structure (in that case fluorination of the surfactant chains) leads to bulkier surfactants (larger Φ) and promotes stable microemulsion formation under mild experimental conditions (in that case temperature and pressure).

Here, surfactant performance is addressed from another perspective by systematically increasing the number of aromatic groups from 0 to 3, using the surfactants shown in Fig. 1 (SDS, SDBS, DC3Ph2 and TC3Ph3). In previous work, surfactants from this group have been used to stabilize dispersions of graphene nanoplatelets (GNPs) in natural rubber latex (NRL) nanocomposites [6], which were investigated using small-angle neutron scattering (SANS). It was seen that surfactants bearing a greater number of aromatic groups gave better quality nanocomposites and higher electrical conductivities. The aim of this new study is to explore the effect of increasing the number of aromatic moieties on interfacial space filling in terms of the surface coverage index Φ, and to explore the effect of Φ on graphene dispersion stability. The surfactant headgroup areas needed as inputs for the calculation of Φ were determined using surface tension measurements at air–water interfaces; further details and the justification of the model are provided and discussed below.

It is hypothesized that Φ plays a significant role in determining surfactant efficiency at graphene surfaces, and hence dispersion stability. Stubby surfactants with multiple aromatic groups are expected to have increased affinity for graphene surfaces. Highlighted for the first time here are the effects of aromatic rings on surfactant coverage, as well as a correlation between coverage and the ability of surfactants to stabilize electrically conductive nanocomposites. Although there are only a limited number of different surfactants used, it is clear that Φ can be used as a guideline for designing new, efficient surfactants for applications in graphene materials science.

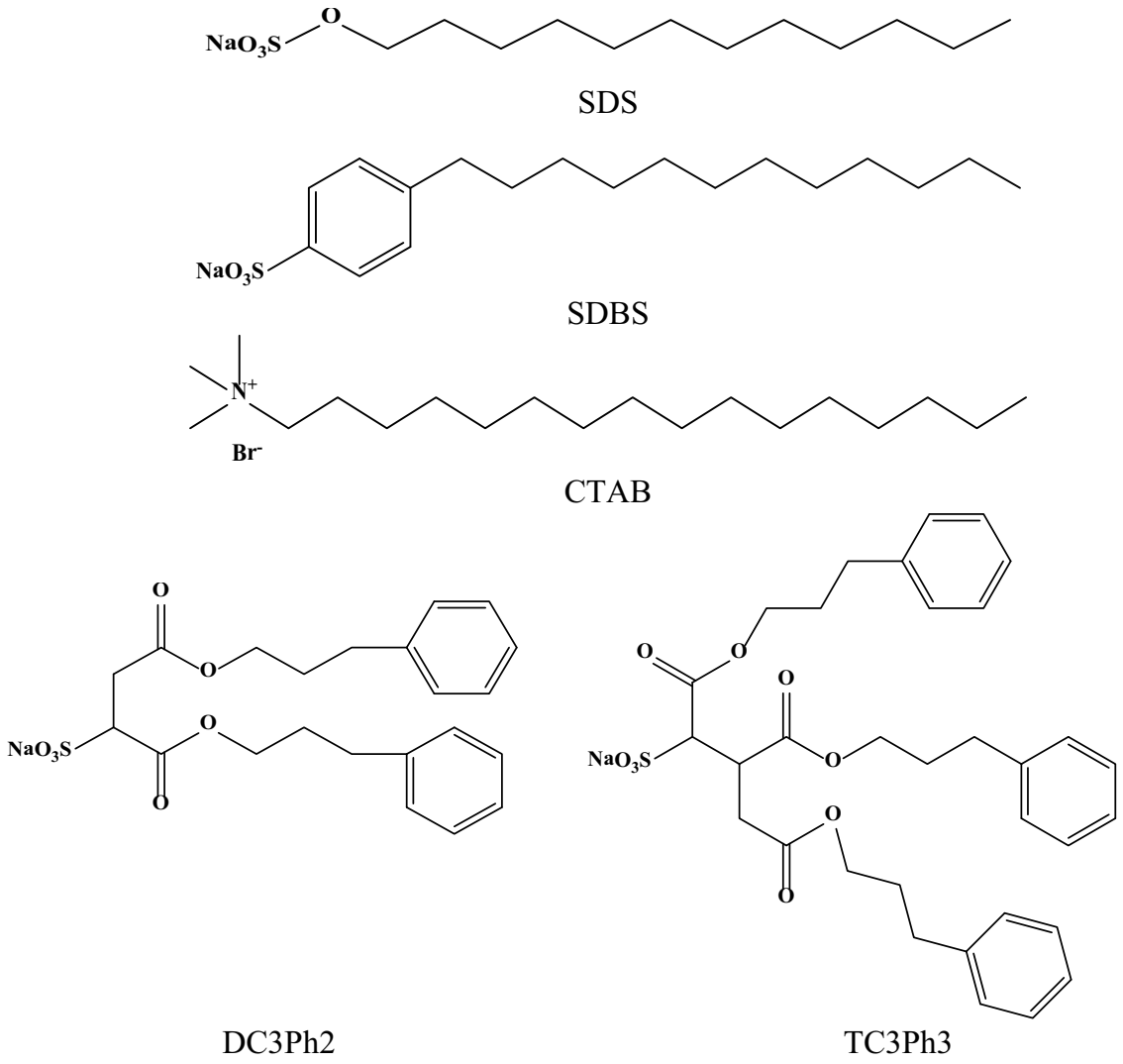

Fig. 1. Molecular structures of surfactants used in this study: SDS (sodium dodecylsulfate), SDBS (sodium dodecylbenzenesulfonate), CTAB (cetyltrimethylammonium bromide), DC3Ph2 (sodium 1,4-dioxo-1,4-bis(3-phenylpropoxy)butane-2-sulfonate), TC3Ph3 (sodium 1,5-dioxo-1,5-bis(3-phenylpropoxy)-3-((3-phenylpropoxy)carbonyl) pentane-2-sulfonate).

2. Material and methods

2.1. Materials

SDS (99%) and SDBS surfactant (98%) were obtained from Sigma Aldrich and used as received. TC3Ph3 and DC3Ph2 surfactants were custom-made and synthesized as detailed previously [6]. The synthesized surfactants were characterized by ^{1}H NMR Spectroscopy. Graphene nanoplatelets (GNPs, average thickness 0.98–3.54 nm) were obtained from UGENT Tech Pte Ltd.

2.2. Air-water (a/w) surface tension measurements

Surface tensions of aqueous surfactant solutions and surfactant-stabilized graphene dispersions were determined using a Wilhelmy tensiometer (CBVP-Z, Kyowa Interface Science) equipped with a platinum plate, at 25 °C. Stock surfactant solutions were diluted to give appropriate concentrations. Using the same surfactant concentrations, graphene dispersions were prepared by adding GNPs at 6 mg/mL and then ultrasonicating for 30 min. The critical micelle concentrations were obtained from the break-points of plots of surface tension (γ) versus ln (surfactant concentration) and also for graphene dispersions.

2.3. Small-angle neutron scattering

Scattering was measured on the ZOOM and LOQ diffractometers at the ISIS Pulsed Neutron and Muon Source, UK. The accessible Q range was 0.007 – 0.23 Å^{-1}, arising from incident neutron wavelengths of λ = 2.2–10 Å at 25 Hz. The SANS samples were prepared in deuterium oxide (D_2O) to enhance the neutron contrast and improve signal-to-noise. The samples at 0.03 M surfactant concentration were contained in 2 mm path length quartz cells and held in a thermostatted computer-controlled sample changer at 25 °C. Absolute scattering intensities *I(Q)* (cm^{-1}) were determined to within 5% by measuring the scattering from a partially-deuterated polymer standard of known molecular weight and hence known *I(0)*. The instrument-independent SANS data, reduced using the Mantid framework (https://www.mantidproject.org), were then model-fit using the SasView program (https://www.sasview.org) constraining scattering length densities (listed on Table S1) and other known parameters. Unknown structural parameters were allowed to refine during the fitting process

to obtain an optimized fit as required by the different scattering model functions. The SANS data are presented as a function of the (magnitude of) scattering vector, $Q = (4\pi/\lambda)\sin(\theta)$, where θ is half of the scattering angle. As a general rule of thumb, the approximate size of a feature is $2\pi/Q$.

3. Results and discussion

3.1. Surfactant self – Assembly and stabilization of graphene dispersions

SANS experiments were performed to determine the shape and size of aggregates in these systems. Fig. 2 shows the SANS profiles for SDS, SDBS, DC3Ph2, and TC3Ph3 surfactants in surfactant solutions and graphene nanoplatelet (GNP) dispersions. The SANS profiles for the surfactant solutions are indicative of charged micelles. SDS and SDBS micelles were fitted with a scattering law describing charged spherical micelle whereas for DC3Ph2 and TC3Ph3 the model for charged ellipsoidal micelles was employed. A more detailed comparison between the measured and literature values can be found in previous work [6,7]. Now with added GNP, the SANS of SDS and SDBS micelles did not indicate any significant changes in micelle shape, with the radius only differing by ~4 Å (see Table 1). On the other hand, for DC3Ph2 the SANS curve is still a characteristic of ellipsoidal micelles with commensurate changes in both polar and equatorial radii. In this case, the surfactants might be both adsorbed on GNP surfaces and aggregated in micelles. Analysis of SANS for TC3Ph3 indicated an ellipsoid-to-stacked disk transition, consistent with adsorption of TC3Ph3 surfactant on the surface of GNPs. Studies by Yoonessi et al. [29] and Milner et al. [30] are consistent with this interpretation, their analyses of GNP scattering data indicated stacked-disk structures with radii of 1250 Å and 2.08 μm.

A convenient way to evaluate the efficiency of surfactants for stabilizing graphene dispersions is by comparing the properties of the surfactant-GNP nanocomposites with pure graphene dispersions. Electrical conductivity measurements of GNPs dispersed in natural rubber latex (NRL) composites showed a trend of increasing electrical conductivity (σ) for surfactants with a higher number of aromatic moietes: GNP/NRL/TC3Ph3 > GNP/NRL/DC3Ph2 > GNP/NRL/SDBS > GNP/NRL/SDS. Interestingly, the highest σ for each nanocomposite was not achieved at the same surfactant concentration, and an optimum surfactant concentration for dispersing graphene was found in each case. The GNP/NRL nanocomposites stabilized with TC3Ph3 achieved the highest σ at 0.016 M (2.22×10^{-5} S cm^{-1}), whereas with DC3Ph2 the optimum concentration was 0.032 M ($\sigma \sim 9.36 \times 10^{-6}$ S cm^{-1}) and for SDBS it was 0.024 M (3.55×10^{-5} S cm^{-1}). The standard surfactant SDS achieved its highest conductivity ($\sigma \sim 1.76 \times 10^{-8}$) at 0.032 M.

The electrical conductivity of nanocomposites is an indication of GNP dispersion quality and stability. Zeta (ζ) – potential measurements of aqueous GNP dispersions with surfactants are listed in Table 1. The results reveal a trend of increasing ζ on increasing the number of aromatic groups in the surfactant chains. Hence, TC3Ph3 gave the highest ζ of – 95 mV, followed by DC3Ph2 (–69 mV), SDS (–43 mV), and SDBS (–40 mV). For all surfactants shown in Fig. 3 it is now possible to draw a relationship between aromaticity, surfactant self-assembly, colloidal stability, and nanocomposite electrical conductivity (SDS is not included because it is a non-aromatic surfactant). It can be seen that changes in surfactant molecular structure, by increasing the num-

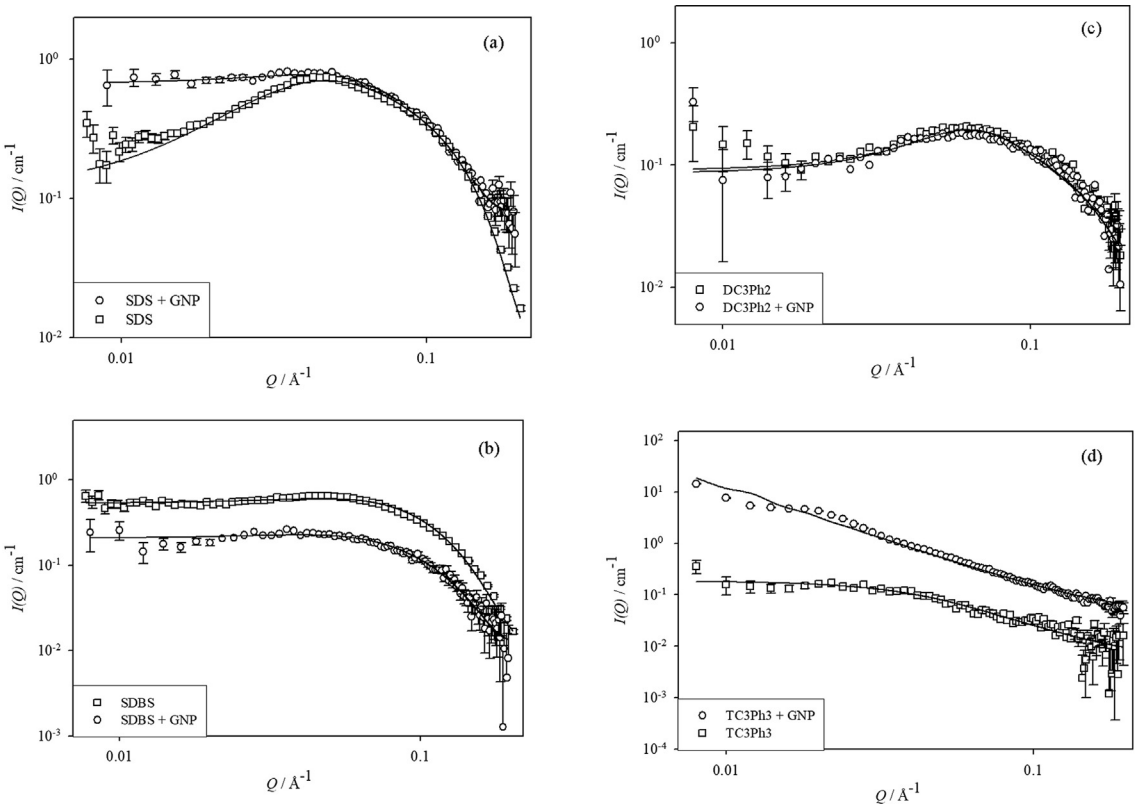

Fig. 2. SANS profiles for surfactant solutions and surfactant-stabilized GNP dispersions for: (a) SDS, (b) SDBS, (c) DC3Ph2, and (d) TC3Ph3. [Surfactant] = 0.03 M and T = 25 °C. Data for SDS and SDBS solution are new to this study; those for other samples are replotted from Ref. [6]. Lines are model fits for charged spherical and ellipsoidal micelles (with an effective Hayter-Penfold $S(Q)$), or stacked disk model (TC3Ph3 + GNP only). Characteristic error bars are shown for the lowest intensity samples. Measurements were done in triplicate.

Table 1
Zeta (ζ) – potential and parameters fit to the SANS data.[a]

Sample	Shape	R^{b} (Å) ± 2 Å	$R_a{}^{c}$ (Å) ± 2 Å	$R_b{}^{c}$ (Å) ± 2 Å	$R_{disk}{}^{d}$ (Å) ± 50 Å	Zeta (ζ) – potential (mV)
SDS	Sphere	20	–	–	–	–
SDBS	Sphere	18	–	–	–	–
DC3Ph2	Ellipsoid	–	5	24	–	–
TC3Ph3	Ellipsoid	–	5	32	–	–
SDS + GNP	Sphere	24	–	–	–	−43 ± 4
SDBS + GNP	Sphere	22	–	–	–	−40 ± 8
DC3Ph2 + GNP	Ellipsoid	–	25	15	–	−69 ± 7
TC3Ph3 + GNP	Stacked disk	–	–	–	286	−95 ± 6

[a] [surf.] = 0.030 M.
[b] R = Radius of spherical micelle.
[c] R_a = polar radius for ellipsoid; R_b = equatorial radius for ellipsoid.
[d] R_{disk} = Radius of stacked disk micelle. Experimental uncertainties correspond to triplicate repeat measurements for SANS and 8 measurements for zeta potential.

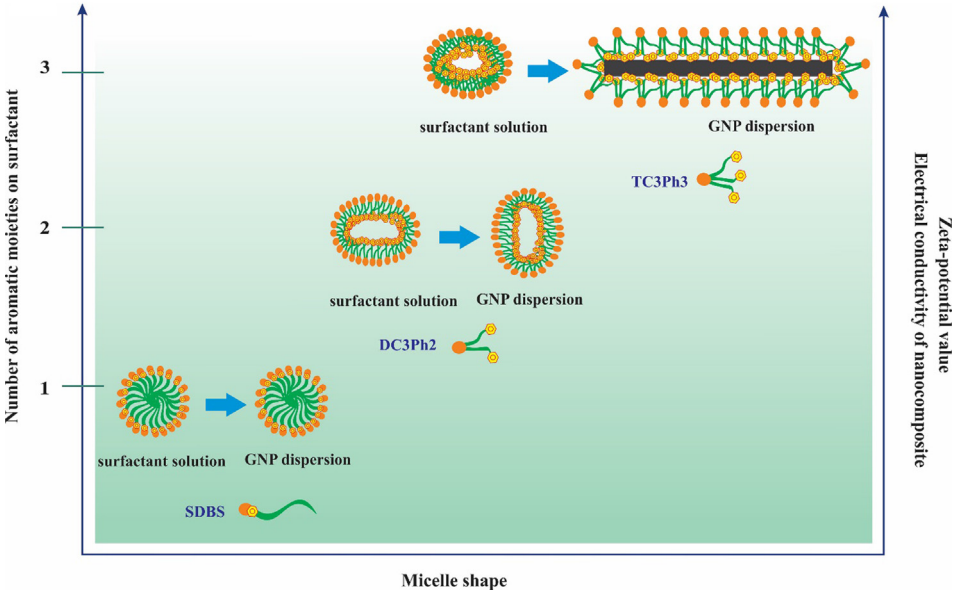

Fig. 3. Increasing the number of aromatic moieties in the surfactants used to stabilize GNP dispersions effects micelle shape, colloidal stability, and properties of the resulting nanocomposites.

ber of aromatic groups, affect compatibility with GNPs. This suggests that the surfactant molecular area might be linked to stability of the GNP dispersions and hence the properties of nanocomposites.

3.2. Surface tension measurements of surfactant-graphene composites at the air–water interface

It is known that surface energy of a material can be obtained through surface tension measurements [31]. Relating to these graphene dispersions, it can be considered that a dispersion would be stable when surfactants can interact favorably with the graphene surfaces and aqueous phase [32–34]. In another challenging application of surfactants, for stabilizing water-in-CO_2 (w/CO_2) microemulsions, it has been established that there is a correlation between the ability of a surfactant to lower the air–water surface tension and performance in stabilizing w/CO_2 microemulsions [35,36]. This approach has been employed to screen solvents for efficient liquid-phase exfoliation [33,34,37] and the state of dispersed carbon materials [38]. In this study, the emphasis is on lowering surface tension between air–water interfaces as a guide for the graphene-water interface (which is expected to be experimentally challenging).

Plots of surface tension versus ln (surfactant concentration), shown in Fig. 4, display the surface tension of pure surfactant solutions and surfactant-stabilized GNP dispersions. The curves demonstrate clean breaks at critical micelle concentrations (cmcs). A slight decay observed after the cmc is noted, as typically encountered with anionic surfactants due to ionic strength effects at higher surfactant concentrations [39]. Quadratics were fitted to the pre-cmc curves using the Gibbs equation to generate adsorption isotherms (Γ) (Eq. (2)) and limiting areas per molecule at cmc ($A_{cmc;}$ Eq. (3)) as follows.

$$\Gamma = -\frac{1}{mRT}\frac{d\gamma}{\ln c} \tag{2}$$

$$A_{cmc} = \frac{1}{\Gamma N_A} \tag{3}$$

Table 2 compiles the values of cmc, surface tension at the cmc (limiting surface tension), and A_{cmc} obtained from the tensiometric analysis.

Changes of surfactant molecular structure, such as varying the length, branching, methylation or aromatization on the surfactant tails, have important effects on the aqueous properties [40–42]. Compared to the literature values (see Supplementary Material

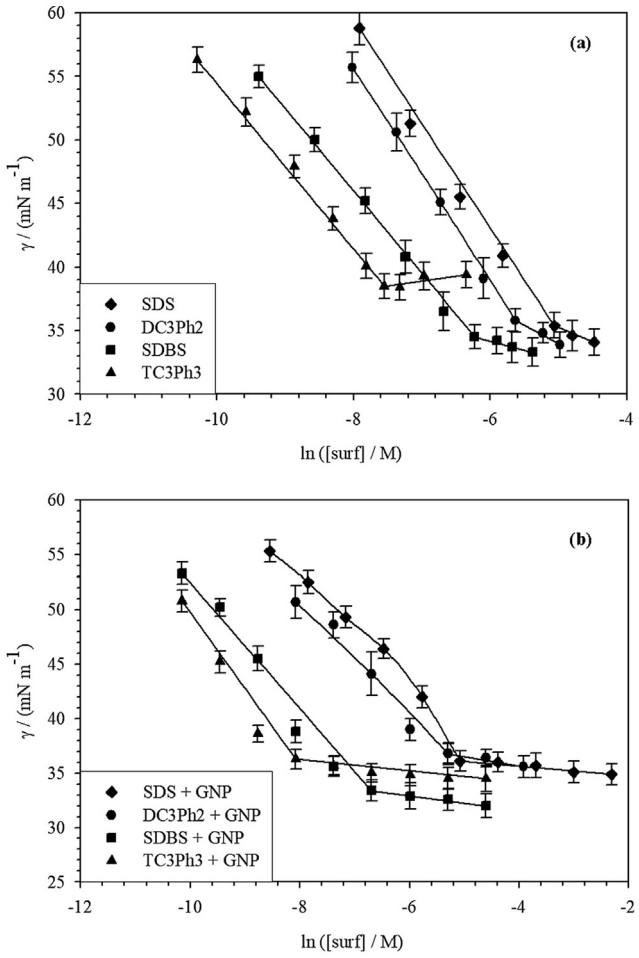

Fig. 4. Air-water surface tension (γ) vs. ln concentration plots of single-, double-, and triple-chain surfactants for: (a) surfactant solutions and (b) GNP dispersion at 25 °C. Lines are quadratic fits to the pre-cmc data. Linear fits to post-cmc data. The error bars represent the uncertainty for triplicate measurements of air–water surface tension.

Table S2), the measured cmc for SDS in this study is noticeably lower, while SDBS is a little higher. Looking at the cmc values it is apparent that there is an increasing hydrophobicity (lower cmc) trend on addition of phenyl rings to the surfactant tails. The TC3Ph3 surfactant has three times the number of aromatic groups compared to SDBS and has a cmc almost one sixth of that for SDBS. On the other hand, the cmc of DC3Ph2 is slightly higher than SDBS indicating it is slightly more hydrophilic. The relative hydrophobicity of a phenyl group has been attributed to about 3.5 normal methylene (CH_2) groups [42]. If an effective chain length (i.e. the total number of carbons in the longest portion only) concept is used to rationalize the higher cmc observed for DC3Ph2, it is not a surprise then that the SDBS can be considered to be more hydrophobic, since SDBS has a total of 16 CH_2 groups where DC3Ph2 only has 6.

Another interesting parameter obtained from the surface tension data analysis is the limiting surface tension at the cmc (γ_{cmc}): surfactants with lower γ_{cmc} values are expected to be better stabilizers. However, it can be seen here that introduction of phenyl groups increases γ_{cmc} with the highest value being for TC3Ph3. This may be attributed to the delocalized electrons in phenyl groups which limit the effectiveness of surfactants [42]. The effect of γ_{cmc} for dispersing graphene is difficult to identify: SDBS should outperform TC3Ph3, but when comparing the zeta potentials and electrical conductivities σ of the nanocomposites it seems not to be the whole story. On the other hand, for the A_{cmc}, there are subtle changes observed. From a molecular geometric viewpoint, addition of phenyl groups enlarges the effective molecular volume in the surfactant tail regions as compared to simple linear alkyl chains. Hence A_{cmc} is expected to increase with a greater number of phenyl groups [42].

Work with a series of phenyl tipped analogues of Aerosol-OT (AOT) showed an increase in the surfactant tail volume with phenyl moieties in comparison to saturated and branched alkyl chains [42]. The values of cmc, γ_{cmc} and A_{cmc} for the phenyl-tipped AOT-analogues surfactants are given in Table S3. The cmc of DC3Ph2 compares well with literature values for double chain phenyl-tipped Aerosol-OT (AOT) analogue surfactants in Table S3. In that study [38], A_{cmc} varied based on the aromatic ring position in the surfactant tails. All in all, extension of the alkyl-phenyl chain length affects the hydrophobicity and effectiveness at lowering surface tension.

Moving now to the GNP dispersions, Table 2 shows that the interfacial properties resemble those for pure surfactant solutions, implying that the presence of GNPs in the system does not significantly control the activity of surfactant at air–water interface (for the most part). Similar observations were found when studying single walled nanotube dispersions in SDS solutions using tensiometry [38,43]. By means of a conductometric titration, Hsieh and co-workers documented a similar micellization point for SDS in water and graphene dispersions [44]. All these observations suggest that air–water surface tension measurements can be used to gauge surfactant interfacial activity for graphene dispersions. Tensiometric analysis of surfactant solutions therefore will be used to assess surfactant interfacial adsorption as discussed in the following section.

Table 2
Parameters[a] derived from air-water (a/w) surface tension measurements and Langmuir isotherm analyses.

Sample	cmc ± 0.03 (×10^{-3} M)	γ_{cmc} ± 1 (mN m^{-1})	A_{cmc} ± 2 (Å^2)	C_1[b] ± 0.03 (×10^{-3} M)	Γ[b] (× 10^{-6}mol m^{-2})	Γ_m (× 10^{-6}mol m^{-2})	θ	θ_{cmc}	C_{opt}[c] ± 0.8 (×10^{-3} M)
SDS	6.28	35.4	93	11.37	1.92 ± 0.14	1.98	0.97 ± 0.01	0.94 ± 0.07	–
SDBS	1.98	34.5	97	3.42	1.59 ± 0.35	1.62	0.98 ± 0.02	0.94 ± 0.05	–
DC3Ph2	3.59	35.8	95	7.00	1.76 ± 0.19	1.77	0.99 ± 0.06	0.99 ± 0.04	–
TC3Ph3	0.53	38.5	100	2.01	1.77 ± 0.21	1.77	1.00 ± 0.10	0.88 ± 0.08	–
SDS + GNP	6.25	36.1	103	50.00	2.25 ± 0.16	2.47	0.91 ± 0.12	0.65 ± 0.19	32.0
SDBS + GNP	1.25	33.4	101	10.00	1.82 ± 0.24	1.91	0.95 ± 0.11	0.86 ± 0.13	24.0
DC3Ph2 + GNP	5.00	36.8	83	20.00	2.71 ± 0.70	2.87	0.95 ± 0.24	0.70 ± 0.10	32.0
TC3Ph3 + GNP	0.31	36.3	70	10.00	3.81 ± 0.75	3.83	0.99 ± 0.04	0.62 ± 0.13	16.0

[a] cmc: critical micelle concentration; γ_{cmc}**:** limiting surface tension at cmc; A_{cmc}: headgroup area at cm**c**; C^1: surfactant concentration in bulk phase; Γ: surface excess density; Γ_m: surface concentration of monolayer; θ surface coverage; θ_{cmc}: surface coverage at the cmc.
[b] At optimum surface coverage.
[c] Surfactant concentration at highest electrical conductivity of nanocomposite. Error estimations based on triplicate measurements.

3.3. Surfactant adsorption: Langmuir isotherm model

It can be expected that there is a dynamic equilibrium between surfactant molecules in the bulk, surfactant molecules at the air–water interface and those that adsorbed on the graphene surfaces. Based on simulations, ionic surfactants adsorbed at graphene surfaces can be thought of as organized structures of surfactant monolayers [45–47]. This is consistent with the interpretation of SANS data given above, where surfactant monolayers are formed around GNPs [6].

The Langmuir isotherm can be used to model equilibrium adsorption from a bulk solution to a monolayer [31]. One way to characterize the monolayer adsorption is to consider the surface excess (Γ). The surface excess can be estimated reliably from the surface tension data via the Gibbs equation (Eq. (2)) for surfactants and with dispersed carbon materials [38,43,44]. The data were then fitted to the Langmuir isotherm (Eq. (4)) and used to generate the limiting values of surface concentrations Γ_m (mol cm^{-2}) and surface coverages (θ). Where C_1 is the surfactant concentration at bulk phase and a is a constant. Although the purpose is to show how surfactant properties at the air–water interface can be used to estimate the activity in graphene dispersions, comparisons were also made with data for GNP dispersions to directly evaluate any differences. Values for C_1, Γ_m, Γ and θ are summarized in Table 2.

$$\Gamma = \frac{\Gamma_m C_1}{C_1 + a} \tag{4}$$

$$\theta = \frac{\Gamma}{\Gamma_m} \tag{5}$$

Returning to the data in Table 2, the concentration needed to achieve the same surface coverage (θ) is significantly lower for the trichain TC3Ph3 (θ = 1.00, C_1 = 0.002 M) than the di-chain surfactant (DC3Ph2; θ = 0.99, C_1 = 0.007 M). In other words, TC3Ph3 does not require such high concentration to attain full coverage (θ = 1). Here, for SDBS, the interface was found to be 98% covered by surfactant molecules whereas SDS was 97% making it slightly lower than DC3Ph2. It can be deduced that at cmc, not all the interface is fully occupied by surfactant, and that all the surfactants required concentrations > cmc to achieve almost or full coverage according to this Langmuir model (Table 2).

The observed trend for GNP dispersions is the same as for the surfactant solutions, by where the prerequisite C_1 for non-aromatic surfactant SDS is still the highest among the series. Comparing data on the optimum surfactant concentrations to achieve the best electrical conductivity and the concentration needed to form a monolayer (C_1), it can be seen that the optimum surfactant concentration generally is well above C_1, except for SDS. This confirms that surfactant molecules adsorb on graphene surfaces to form monolayers. This will be used below, to develop the surfactant coverage index Φ and help understand how surfactant molecular structure can be correlated with graphene compatibility and dispersion stability.

3.4. Calculation of the surface coverage index (Φ)

Is it possible to quantify the effectiveness of a surfactant for stabilizing the graphene-water interface? To employ calculations of Φ, it is assumed that the surfactant behavior at the air–water interface and on graphene surfaces is similar, the justification was

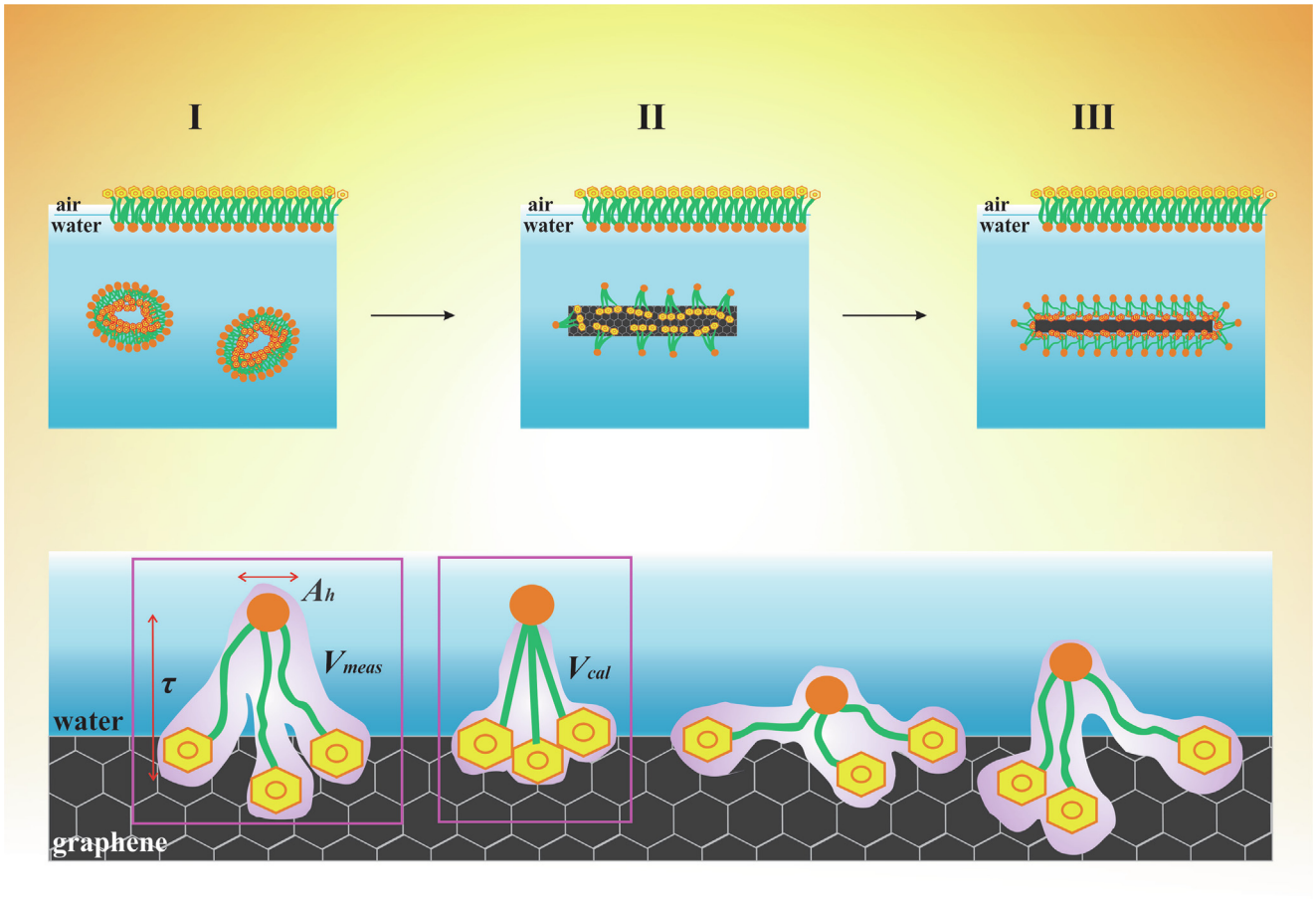

Fig. 5. Schematic illustration of surfactant molecular arrangement on graphene surfaces to visualize how the coverage index is calculated.

Table 3
Calculated surface coverage index (ϕ) correlates with surfactant performance.

System[a]	Φ[b] ± 0.02	Nanocomposites electrical conductivity enhancement[c]	Polymer[d]	Number of aromatic group	Ref
This study					
SDS	0.20	$(1.47 \pm 0.09) \times 10^6$	NRL	0	[6]
SDS + GNP	0.18				
SDBS	0.21	$(2.36 \pm 0.01) \times 10^8$	NRL	1	
SDBS + GNP	0.20				
DC3Ph2	0.32	$(6.21 \pm 0.03) \times 10^8$	NRL	2	
DC3Ph2 + GNP	0.37				
TC3Ph3	0.34	$(1.47 \pm 0.08) \times 10^9$	NRL	3	
TC3Ph3 + GNP	0.49				
Other works					
SDS + TRGO	0.20	1.00×10^6	NRL	0	[52]
SDBS + G	0.21	9.20×10^5	PP	1	[14,53]
CTAB + RGO	0.23	1.00×10^4	NRL	0	[54]
CTAB + MLG	0.23	2.22×10^6	SBR	0	[55]

[a] GNP: graphene nanoplatelet; TRGO: thermally reduced graphene oxide; G: graphene; RGO: reduced graphene oxide; MLG: multilayer graphene.
[b] Coverage index for SDS and SDBS in other works were calculated using data obtained in this study meanwhile A_{cmc} used to calculate Φ for CTAB obtained from[56]
[c] Relative to the electrical conductivity of polymer host. [d]NRL: natural rubber latex; PP: polypropylene; SBR: styrene butadiene rubber. Error estimation based on triplicate measurements.

already discussed previously (Sections 3.2 and 3.3). Hence, under these assumptions, the physical parameters needed to calculate the coverage index can be obtained from the air–water surface tension measurements.

Recalling Eq. (1) above, the proposed index requires calculation of the total volume of the molecular fragments from the literature V_{cal} and the experimentally measured values of surfactant volume at air–water interface as V_{meas} (Eq. (6)) [23,48,49].

$$V_{meas} = A_{cmc}\tau \tag{6}$$

where A_{cmc} is the surfactant headgroup area at the cmc and τ is the interfacial surfactant layer thickness, which can be estimated from the effective tail length by the Tanford equation [23].

$$\tau = 1.5 + 1.265(n_c) \tag{7}$$

where n_c represents the number of carbons in linear chains.

A better estimate of layer thickness may be obtained from computer studies at graphene-water interfaces [47,50] or through scattering experiments, but the purpose here is to simplify the approach, and especially to avoid the need for neutron scattering. The possible arrangement of surfactant tails at a graphene surface is depicted in Fig. 5. As can be seen, the surfactant tail may be tilted or bent relative to the graphene surface to maximise the intermolecular interactions at an optimum configuration or length [51]. Detailed calculations and parameters used for the analysis are found in Supplementary material (Table S4 and S5). Table 3 shows the calculated Φ for SDS, SDBS, DC3Ph2, and TC3Ph3 surfactants. The coverage analysis for the GNP dispersions is also included. To further study the correlation between Φ and surfactant performance for stabilizing graphene dispersions, the value for Φ is included here for a different ionic surfactant which is frequently used in this field (Cetyltrimethylammonium bromide: CTAB, Table 3).

3.5. Coverage index (Φ) and surfactant performance in graphene dispersions

The hydrophobic effect favors the exclusion of surfactant tails from the aqueous phase and drives the adsorption onto graphene [51,57]. Here, the relationship between coverage index and experimental studies of graphene dispersion stability is demonstrated in

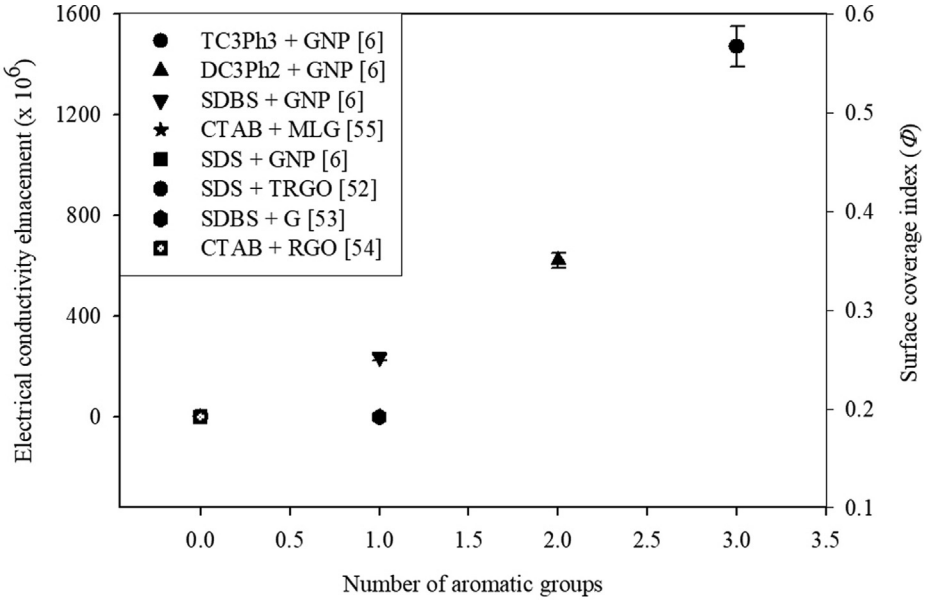

Fig. 6. Correlation between number of aromatic groups in the surfactant, surface coverage index (Φ), and electrical conductivity enhancement of the resulting graphene nanocomposites. The error bars represent the uncertainty of the electrical conductivity enhancement.

Fig. 6. (It is important to note that chemical structural details, being the volume of surfactant tail and headgroup area are not considered for the Langmuir isotherm).

The single chain SDS surfactant has relatively low Φ at its cmc (0.20). The presence of an aromatic moiety near the SDBS headgroup has a small effect on Φ, raising it to 0.21. Introducing a second chain and with now two aromatic rings for DC3Ph2 increases Φ to 0.32 (Table 3). Adding in now a third aromatic group for TC3Ph3 increases Φ to 0.34, which also provides the greatest stability for graphene dispersions. On the other hand, for a linear chain aromatic-free cationic surfactant CTAB the value of Φ is 0.23; above the values for both SDS and SDBS. It is, however, too early to draw a firm conclusion on the effect of surfactant headgroup type (anionic vs cationic) on Φ owing to only limited data used in this study.

Previous work [6], showed correlations between Φ, the optimum electrical conductivity enhancement and stability of graphene/natural rubber composites (NRL): here also, this general trend is seen (see Table 3). In terms of graphene dispersion properties, surfactant performance is improved on increasing the number of aromatic groups in the surfactant (see Fig. 6). The effect is more profound when comparing the single and double-chain surfactants (Fig. 6).

It can be assumed that surfactants with higher coverage index will present as "stubby" molecules at the interface, providing a better barrier against direct penetration of water into the interfacial zone, which would lead to instabilities. Although previous literature using this coverage index Φ was about water-in-CO_2 (w/CO_2) microemulsions, the general trend is that structural modifications leading to higher coverage values will offer improved surfactant performance in any application [21,22,26]. The above results show that the readily calculated index Φ offers a quick and straightforward method in screening surfactant chemical structures for two challenging applications of surfactants: surfactant stabilized graphene dispersions and w/CO_2 microemulsions. Hence, correlations between Φ and dispersion stability and properties of nanocomposites have been highlighted, based on reasonable assumptions about surfactant structure and determination of aqueous properties of surfactant solutions and graphene dispersions.

4. Conclusions

To date, the affinity of aromatic surfactants and polymers for graphenes has been attributed to π-π interactions. Both experimental [5,8,58] and simulation studies [17,18] have shown that increasing the number of aromatic groups in surfactants has notable effects on stability of graphene dispersions. It is of interest to explore whether π-π interactions are the only way to account for graphene compatibility or are there other approaches which might be helpful. Here, a new index for graphene-surfactant compatibility has been introduced and evaluated, which builds in the celebrated packing parameter framework of Israelachvili [24]. This parameter is the surfactant coverage index (Φ) and it has been demonstrated to be useful in describing the compatibility of surfactants to stabilize graphene-water interfaces for aqueous dispersions [6]. The links between surfactant chemical architecture and graphene dispersion stability can be now readily understood, increasing Φ indicates that surfactant molecules will occupy more space at the graphene-water interface, hence preventing penetration of water to the graphene surfaces. This new concept shows great promise in helping guide design of optimized surfactants for graphene-water dispersions and other challenging applications.

CRediT authorship contribution statement

Tretya Ardyani: Investigation, Writing – original draft, Writing – review & editing, Conceptualization. **Azmi Mohamed:** Supervision, Funding acquisition, Project administration, Conceptualization. **Suriani Abu Bakar:** Resources, Methodology. **Masanobu Sagisaka:** Methodology, Formal analysis, Resources. **Mohamad Hafiz Mamat:** Formal analysis, Visualization. **Mohd Khairul Ahmad:** Formal analysis, Visualization. **Sofian Ibrahim:** Formal analysis, Resources. **H.P.S. Abdul Khalil:** Visualization. **Stephen M. King:** Validation, Data curation. **Sarah E. Rogers:** Data curation, Investigation. **Julian Eastoe:** Writing – review & editing, Validation.

Declaration of Competing Interest

The authors declare that they have no known competing financial interests or personal relationships that could have appeared to influence the work reported in this paper.

Acknowledgment

The work funded under grants from Fundamental Research Grant Scheme (Grant Code: FRGS/1/2020/STG04/UPSI/02/1) and NEWTON Fund: Use of ISIS Neutron and Muon Source (Grant Code: 2019-0257-103-11). This project was supported by JSPS [KAKENHI, Grant-in-Aid for Young Scientists (A), No. 23685034], KAKENHI, Grant-in-Aid for Scientific Research (B), No. 26289345, Fund for the Promotion of Joint International Research (Fostering Joint International Research) No. 15KK0221, Grant-in-Aid for Challenging Research (Exploratory), No.17K19002] and Leading Research Organizations (RCUK [through EPSRC EP/I018301/1], ANR [13-G8ME-0003]) under the G8 Research Councils Initiative for Multi-lateral Research Funding—G8-2012. This work benefited from the use of the SasView application, originally developed under NSF Award DMR-0520547. SasView also contains code developed with funding from the EU Horizon 2020 programme under the SINE2020 project Grant No 654000.

Appendix A. Supplementary material

Supplementary data to this article can be found online at https://doi.org/10.1016/j.jcis.2022.03.145.

References

[1] J. Texter, Graphene Dispersions, Curr. Opin. Colloid Interface Sci. 19 (2014) 163–174, https://doi.org/10.1016/j.cocis.2014.04.004.
[2] S. Lin, C.-J. Shih, V. Sresht, A. Govind Rajan, M.S. Strano, D. Blankschtein, Understanding the colloidal dispersion stability of 1D and 2D materials: Perspectives from molecular simulations and theoretical modeling, Adv. Colloid Interface Sci. 244 (2017) 36–53.
[3] Z. Sun, V. Nicolosi, D. Rickard, S.D. Bergin, D. Aherne, J.N. Coleman, Quantitative Evaluation of Surfactant-Stabilized Single-Walled Carbon Nanotubes: Dispersion Quality And Its Correlation With Zeta Potential, J. Phys. Chem. C 112 (2008) 10692–10699, https://doi.org/10.1021/jp8021634.
[4] R.J. Smith, M. Lotya, J.N. Coleman, The Importance of Repulsive Potential Barriers for the Dispersion of Graphene using Surfactants, New J. Phys. 12 (2010), https://doi.org/10.1088/1367-2630/12/12/125008 125008.
[5] D. Parviz, S. Das, H.S.T. Ahmed, F. Irin, S. Bhattacharia, M.J. Green, Dispersions of Non-Covalently Functionalized Graphene with Minimal Stabilizer, ACS Nano 6 (2012) 8857–8867, https://doi.org/10.1021/nn302784m.
[6] A. Mohamed, T. Ardyani, S. Abu Bakar, M. Sagisaka, Y. Umetsu, J.J. Hamon, B.A. Rahim, S.R. Esa, H.P.S. Khalil, M.H. Mamat, S. King, J. Eastoe, Rational Design of Aromatic Surfactants for Graphene/Natural Rubber Latex Nanocomposites with Enhanced Electrical Conductivity, J. Colloid Interface Sci. 516 (2018) 34–47, https://doi.org/10.1016/j.jcis.2018.01.041.
[7] T. Ardyani, A. Mohamed, S.A. Bakar, M. Sagisaka, Y. Umetsu, M.H. Mamat, M.K. Ahmad, H.P.S. Abdul Khalil, S. King, S.E. Rogers, J. Eastoe, Surfactants with Aromatic Headgroups For Optimizing Properties of Graphene/Natural Rubber Latex Composites (NRL): Surfactants with Aromatic Amine Polar Heads, J. Colloid Interface Sci. 545 (2019) 184–194, https://doi.org/10.1016/j.jcis.2019.03.012.
[8] L. Zhang, Z. Zhang, C. He, L. Dai, J. Liu, L. Wang, Rationally Designed Surfactants for Few-Layered Graphene Exfoliation: Ionic Groups Attached to Electron-Deficient π-Conjugated Unit through Alkyl Spacers, ACS Nano 8 (2014) 6663–6670, https://doi.org/10.1021/nn502289w.

[9] C. Backes, T.M. Higgins, A. Kelly, C. Boland, A. Harvey, D. Hanlon, J.N. Coleman, Guidelines for Exfoliation, Characterization and Processing of Layered Materials Produced by Liquid Exfoliation, Chem. Mater. 29 (2017) 243–255, https://doi.org/10.1021/acs.chemmater.6b03335.
[10] A. Mohamed, T. Ardyani, S.A. Bakar, P. Brown, M. Hollamby, M. Sagisaka, J. Eastoe, Graphene-philic Surfactants for Nanocomposites in Latex Technology, Adv. Colloid Interface Sci. 230 (2016) 54–69, https://doi.org/10.1016/j.cis.2016.01.003.
[11] K.W.J. Heard, C. Bartlam, C.D. Williams, J. Zhang, A.A. Alwattar, M.S. Little, A.V. S. Parry, F.M. Porter, M.A. Vincent, I.H. Hillier, F.R. Siperstein, A. Vijayaraghavan, S.G. Yeates, P. Quayle, Initial Studies Directed toward the Rational Design of Aqueous Graphene Dispersants, ACS Omega 4 (2019) 1969–1981, https://doi.org/10.1021/acsomega.8b03147.
[12] E. Tkalya, M. Ghislandi, A. Alekseev, C. Koning, J. Loos, Latex-based Concept For The Preparation Of Graphene-Based Polymer Nanocomposites, J. Mater. Chem. 20 (2010) 3035–3039, https://doi.org/10.1039/b922604d.
[13] M. Lotya, Y. Hernandez, P.J. King, R.J. Smith, V. Nicolosi, L.S. Karlsson, F.M. Blighe, S. De, Z. Wang, I.T. McGovern, G.S. Duesberg, J.N. Coleman, Liquid Phase Production of Graphene by Exfoliation of Graphite in Surfactant/Water Solutions, J. Am. Chem. Soc. 131 (2009) 3611–3620, https://doi.org/10.1021/ja807449u.
[14] M. Ghislandi, E. Tkalya, B. Marinho, C.E. Koning, G. de With, Electrical Conductivities Of Carbon Powder Nanofillers And Their Latex-Based Polymer Composites, Compos. Part A Appl. Sci. Manuf. 53 (2013) 145–151, https://doi.org/10.1016/j.compositesa.2013.06.008.
[15] X. An, T. Simmons, R. Shah, C. Wolfe, K.M. Lewis, M. Washington, S.K. Nayak, S. Talapatra, S. Kar, "Stable Aqueous Dispersions of Noncovalently Functionalized Graphene from Graphite and their Multifunctional High-Performance Applications, Nano Lett. 10 (2010) 4295–4301, https://doi.org/10.1021/nl903557p.
[16] Y. Shin, X. Just-Baringo, M. Boyes, A. Panigrahi, M. Zarattini, Y. Chen, X. Liu, G. Morris, E. Prestat, K. Kostarelos, S. Vranic, I. Larrosa, C. Casiraghi, Enhanced Liquid Phase Exfoliation Of Graphene In Water Using An Insoluble Bis-Pyrene Stabiliser, Faraday Discuss. 227 (2021) 46–60, https://doi.org/10.1039/C9FD00114J.
[17] J. Björk, F. Hanke, C.-A. Palma, P. Samori, M. Cecchini, M. Persson, Adsorption of Aromatic and Anti-Aromatic Systems on Graphene through π−π Stacking, J. Phys. Chem. Lett. 1 (2010) 3407–3412, https://doi.org/10.1021/jz101360k.
[18] S. Glanzer, A.F. Sax, Carbon Nanotubes Dressed By Aromatic Molecules, Mol. Phys. 111 (2013) 2427–2438, https://doi.org/10.1080/00268976.2013.831499.
[19] E.M. Pérez, N. Martín, π–π Interactions In Carbon Nanostructures, Chem. Soc. Rev. 44 (2015) 6425–6433, https://doi.org/10.1039/C5CS00578G.
[20] A. Mohamed, K. Trickett, S.Y. Chin, S. Cummings, M. Sagisaka, L. Hudson, S. Nave, R. Dyer, S.E. Rogers, R.K. Heenan, J. Eastoe, Universal Surfactant for Water, Oils, and CO2, Langmuir 26 (17) (2010) 13861–13866.
[21] A. Mohamed, M. Sagisaka, F. Guittard, S. Cummings, A. Paul, S.E. Rogers, R.K. Heenan, R. Dyer, J. Eastoe, Low Fluorine Content CO_2-philic Surfactants, Langmuir 27 (2011) 10562–10569, https://doi.org/10.1021/la2021885.
[22] M.T. Stone, P.G. Smith, S.R.P. da Rocha, P.J. Rossky, K.P. Johnston, Low Interfacial Free Volume of Stubby Surfactants Stabilizes Water-in-Carbon Dioxide Microemulsions, J. Phys. Chem. B 108 (2004) 1962–1966, https://doi.org/10.1021/jp036224w.
[23] C. Tanford, Micelle shape and size, J. Phys. Chem. 76 (21) (1972) 3020–3024.
[24] J.N. Israelachvili, D.J. Mitchell, B.W. Ninham, Theory of Self-Assembly of Hydrocarbon Amphiphiles into Micelles and Bilayers, J. Chem. Soc., Faraday Trans. 72 (1976) 1525–1568, https://doi.org/10.1039/F29767201525.
[25] M.T. Stone, S.R.P. da Rocha, P.J. Rossky, K.P. Johnston, Molecular Differences between Hydrocarbon and Fluorocarbon Surfactants at the CO_2/Water Interface, J. Phys. Chem. B 107 (2003) 10185–10192, https://doi.org/10.1021/jp035422k.
[26] R. Nagarajan, Molecular Packing Parameter and Surfactant Self-Assembly: The Neglected Role of the Surfactant Tail, Langmuir 18 (2002) 31–38, https://doi.org/10.1021/la010831y.
[27] G. Sun, G. Chen, J. Liu, J. Yang, J. Xie, Z. Liu, R. Li, X. Li, A Facile Gemini Surfactant-Improved Dispersion of Carbon Nanotubes in Polystyrene, Polymer 50 (2009) 5787–5793, https://doi.org/10.1016/j.polymer.2009.10.007.
[28] A. Mohamed, M. Sagisaka, M. Hollamby, S.E. Rogers, R.K. Heenan, R. Dyer, J. Eastoe, Hybrid CO_2-philic Surfactants with Low Fluorine Content, Langmuir 28 (2012) 6299–6306, https://doi.org/10.1021/la3005322.
[29] M. Yoonessi, J.R. Gaier, Highly Conductive Multifunctional Graphene Polycarbonate Nanocomposites, ACS Nano 4 (2010) 7211–7220, https://doi.org/10.1021/nn1019626.
[30] E.M. Milner, N.T. Skipper, C.A. Howard, M.S.P. Shaffer, D.J. Buckley, K.A. Rahnejat, P.L. Cullen, R.K. Heenan, P. Lindner, R. Schweins, Structure and Morphology of Charged Graphene Platelets in Solution by Small-Angle Neutron Scattering, J. Am. Chem. Soc. 134 (2012) 8302–8305, https://doi.org/10.1021/ja211869u.
[31] M.J. Rosen, Surfactant and Interfacial Phenomena, third ed., John Wiley & Sons, New Jersey, 2004.
[32] J.N. Coleman, Liquid-Phase Exfoliation of Nanotubes and Graphene, Adv. Funct. Mater. 19 (2009) 3680–3695, https://doi.org/10.1002/adfm.200901640.
[33] J. Shen, Y. He, J. Wu, C. Gao, K. Keyshar, X. Zhang, Y. Yang, M. Ye, R. Vajtai, J. Lou, P.M. Ajayan, Liquid Phase Exfoliation of Two-Dimensional Materials by Directly Probing and Matching Surface Tension Components, Nano Lett. 15 (2015) 5449–5454, https://doi.org/10.1021/acs.nanolett.5b01842.
[34] Y. Hernandez, V. Nicolosi, M. Lotya, F.M. Blighe, Z. Sun, S. De, I.T. McGovern, B. Holland, M. Byrne, Y.K. Gun'Ko, J.J. Boland, P. Niraj, G. Duesberg, S. Krishnamurthy, R. Goodhue, J. Hutchison, V. Scardaci, A.C. Ferrari, J.N. Coleman, High-Yield Production of Graphene by Liquid-Phase Exfoliation of Graphite, Nat. Nanotechnol. 3 (9) (2008) 563–568.
[35] J. Eastoe, A. Paul, A. Downer, D.C. Steytler, E. Rumsey, Effects of Fluorocarbon Surfactant Chain Structure on Stability of Water-in-Carbon Dioxide Microemulsions. Links between Aqueous Surface Tension and Microemulsion Stability, Langmuir 18 (2002) 3014–3017, https://doi.org/10.1021/la015576w.
[36] M. Sagisaka, S. Iwama, S. Hasegawa, A. Yoshizawa, A. Mohamed, S. Cummings, S.E. Rogers, R.K. Heenan, J. Eastoe, Super-Efficient Surfactant for Stabilizing Water-in-Carbon Dioxide Microemulsions, Langmuir 27 (10) (2011) 5772–5780.
[37] J. Shen, J. Wu, M. Wang, P. Dong, J. Xu, X. Li, X. Zhang, J. Yuan, X. Wang, M. Ye, R. Vajtai, J. Lou, P.M. Ajayan, Surface Tension Components Based Selection of Cosolvents for Efficient Liquid Phase Exfoliation of 2D Materials, Small 12 (2016) 2741–2749, https://doi.org/10.1002/smll.201503834.
[38] V. Sa, K.G. Kornev, Analysis of Stability of Nanotube Dispersions Using Surface Tension Isotherms, Langmuir 27 (22) (2011) 13451–13460.
[39] J. Eastoe, S. Nave, A. Downer, A. Paul, A. Rankin, K. Tribe, J. Penfold, Adsorption of Ionic Surfactants at the Air-Solution Interface, Langmuir 16 (2000) 4511–4518, https://doi.org/10.1021/la991564n.
[40] S. Nave, J. Eastoe, J. Penfold, What Is So Special about Aerosol-OT? 1. Aqueous Systems, Langmuir 16 (2000) 8733–8740, https://doi.org/10.1021/la000341q.
[41] S. Nave, J. Eastoe, R.K. Heenan, D. Steytler, I. Grillo, What Is So Special about Aerosol-OT? Part III – Glutaconate versus Sulfosuccinate Headgroups and Oil-Water Interfacial Tensions, Langmuir 18 (2002) 1505–1510, https://doi.org/10.1021/la015564a.
[42] S. Nave, A. Paul, J. Eastoe, A.R. Pitt, R.K. Heenan, What Is So Special about Aerosol-OT? Part IV. Phenyl-Tipped Surfactants, Langmuir 21 (2005) 10021–10027, https://doi.org/10.1021/la050767a.
[43] N. Grossiord, P. van der Schoot, J. Meuldijk, C.E. Koning, Determination of The Surface Coverage of Exfoliated Carbon Nanotubes by Surfactant Molecules in Aqueous Solution, Langmuir 23 (2007) 3646–3653, https://doi.org/10.1021/la062684f.
[44] A.G. Hsieh, C. Punckt, S. Korkut, I.A. Aksay, Adsorption of Sodium Dodecyl Sulfate on Functionalized Graphene Measured by Conductometric Titration, J. Phys. Chem. B 117 (2013) 7950–7958, https://doi.org/10.1021/jp403876t.
[45] S. Manne, J.P. Cleveland, H.E. Gaub, G.D. Stucky, P.K. Hansma, Direct Visualization of Surfactant Hemimicelles by Force Microscopy of The Electrical Double Layer, Langmuir 10 (1994) 4409–4413, https://doi.org/10.1021/la00024a003.
[46] E.J. Wanless, W.A. Ducker, Organization of Sodium Dodecyl Sulfate at The Graphite-Solution Interface, J. Phys. Chem. 100 (1996) 3207–3214, https://doi.org/10.1021/jp952439x.
[47] H. Sun, X. Yang, Molecular Simulation of Self-Assembly Structure and Interfacial Interaction for SDBS Adsorption on Graphene, Colloids Surf. A 462 (2014) 82–89, https://doi.org/10.1016/j.colsurfa.2014.08.013.
[48] Z.X. Li, J.R. Lu, R.K. Thomas, J. Penfold, Neutron Reflectivity Studies of the Adsorption of Aerosol-OT at the Air-Water Interface: The Structure of the Sodium Salt, J. Phys. Chem. B 101 (1997) 1615–1620, https://doi.org/10.1021/jp962812g.
[49] S.S. Berr, R.R.M. Jones, Small-Angle Neutron Scattering from Aqueous Solutions of Sodium Perfluorooctanoate above the Critical Micelle Concentration, J. Phys. Chem. 93 (1989) 2555–2558, https://doi.org/10.1021/j100343a062.
[50] S. Lin, C.-J. Shih, M.S. Strano, D. Blankschtein, Molecular Insights into the Surface Morphology, Layering Structure, and Aggregation Kinetics of Surfactant-Stabilized Graphene Dispersions, J. Am. Chem. Soc. 133 (2011) 12810–12823, https://doi.org/10.1021/ja2048013.
[51] C. Tanford, The Hydrophobic Effect and the Organization of Living Matter, Science 200 (1978) 1012–1018, https://doi.org/10.1126/science.653353.
[52] H. Aguilar-Bolados, J. Brasero, M.A. Lopez-Manchado, M. Yazdani-Pedram, High Performance Natural Rubber/Thermally Reduced Graphite Oxide Nanocomposites by Latex Technology, Compos. Part B Eng. 67 (2014) 449–454, https://doi.org/10.1016/j.compositesb.2014.08.010.
[53] M. G. Ghislandi, Nano-scaled Carbon Fillers and Their Functional Polymer Composites, PhD Thesis, Technische Universiteit Eindhoven, Eindhoven, 2012, https://doi.org/10.6100/IR733425.
[54] C.F. Matos, F. Galembeck, A.J.G. Zarbin, Multifunctional and Environmentally Friendly Nanocomposites Between Natural Rubber and Graphene or Graphene Oxide, Carbon 78 (2014) 469–479, https://doi.org/10.1016/j.carbon.2014.07.028.
[55] J.S. Kim, J.H. Yun, I. Kim, S.E. Shim, Electrical Properties of Graphene/SBR Nanocomposite Prepared by Latex Heterocoagulation Process at Room Temperature, J. Ind. Eng. Chem. 17 (2011) 325–330, https://doi.org/10.1016/j.jiec.2011.02.034.
[56] F. Golmohammadi, M. Amiri, H. Gharibi, A. Yousefi, M. Safari, Co-solvent Effect on Spontaneous Formation of Large Nanoscale Structures in Catanionic Mixtures in the Anionic-Rich Region, J. Solution Chem. 49 (2020) 16–33, https://doi.org/10.1007/s10953-019-00935-6.
[57] C. Tanford, Interfacial Free Energy and the Hydrophobic Effect, Proc. Natl. Acad. Sci. U. S. A. 76 (1979) 4175–4176, https://doi.org/10.1073/pnas.76.9.4175.
[58] D. Lin, B. Xing, Adsorption of Phenolic Compounds by Carbon Nanotubes: Role of Aromaticity and Substitution of Hydroxyl Groups, Environ. Sci. Technol. 42 (2008) 7254–7259, https://doi.org/10.1021/es801297u.